Dynamics of nonlinearly coupled magnetic-field-aligned electromagnetic electron-cyclotron waves near the zero-group-dispersion point in magnetized plasmas

I. Kourakis[a] and P. K. Shukla[b]
Institut für Theoretische Physik IV and Centre for Plasma Science and Astrophysics, Fakultät für Physik und Astronomie, Ruhr-Universität Bochum, D-44780 Bochum, Germany

G. E. Morfill[c]
Max-Planck Institut für extraterrestrische Physik, Giessenbachstrasse, D-85740 Garching, Germany

(Received 3 May 2005; accepted 16 June 2005; published online 25 July 2005)

The nonlinear coupling between two magnetic-field-aligned electromagnetic electron-cyclotron (EMEC) waves in plasmas is considered. Evaluating the ponderomotive coupling between the EMEC waves and quasistationary plasma density perturbations, a pair of coupled nonlinear Schrödinger equations (CNLSEs) is obtained. The CNLSEs are then used to investigate the occurrence of modulational instability in magnetized plasmas. Waves in the vicinity of the zero-group-dispersion point are considered, so that the group dispersion terms may either bear the same or different signs. It is found that a stable EMEC wave can be destabilized due to its nonlinear interactions with an unstable one, while a pair of unstable EMEC waves yields an increased instability growth rate. Individually stable waves remain stable while interacting with one another. Stationary nonlinear solutions of the coupled equations are presented. The relevance of our investigation to nonlinear phenomena in space plasmas is discussed. © *2005 American Institute of Physics*. [DOI: 10.1063/1.1994747]

I. INTRODUCTION

Electromagnetic electron-cyclotron (EMEC) waves are common in the Earth's magnetosphere.[1,2] They can be excited by various linear instabilities, e.g., caused by electron temperature anisotropy or streaming electron beams. Long-wavelength EMEC waves are known to be excited, for instance, when electromagnetic energy from a lightning strike enters a magnetic-field line duct (this process is more efficient near the magnetic poles). Such electromagnetic energy can be guided along closed magnetic-field lines due to the enhanced ionization usually present near such magnetic-field ducts. The wave then propagates along the magnetic-field lines and can be observed at the opposite pole (conjugate point). Because of the wave's dispersion, different frequencies arrive at a radio receiver, say, at different times, so a descending glide tone can be heard due to lightning strikes occurring in the opposite hemisphere (hence the term *whistlers* used for these waves). Whistlers also occur widely in the plasmasphere, magnetosheath, and terrestrial foreshock.[2] Of particular interest in the following are EMEC-wave-related modulated structures associated with enhanced quasistationary density perturbations, which have most often been observed by recent satellite missions (e.g., Cluster[3] and Freja[4]) in the magnetosphere and in laboratory experiments.[5–7] A comprehensive review of EMEC-wave-related phenomena in both space and experimental physics can be found in Ref. 8.

In principle, as the EMEC wave amplitudes increase, nonlinear effects become significant. One such effect, which is long known to govern wave propagation in dispersive media, is the nonlinear modulation of the carrier wave amplitude due to the parametric coupling with nonresonant low-frequency perturbations. Following the early work of Hasegawa,[9,10] who used a reductive perturbation method to study the self-modulation of EMEC waves by low-frequency magnetohydrodynamic (MHD) perturbations, Karpman and Washimi[11] included the ponderomotive force in the description of the modulation of EMEC waves by low-frequency magnetoacoustic perturbations. Those results were then applied by the same authors to study the amplitude modulation of high-frequency magnetic-field-aligned EMEC waves due to their coupling with slow magnetosonic waves,[12] within a MHD approximation, and the technique was later employed by Shukla and co-workers[13–16] in a description of the parametric interactions between whistlers and ion-acoustic perturbations. Recently, the formalism was adopted as a model for the localized whistler-related envelope structures coupled to density perturbations[17,18] (whistler bisolitons or whistlerons), which are frequently observed in the Earth's magnetosphere. The method was recently also employed in a study of pair (e.g., electron-positron) plasmas,[19] which are believed to exist in pulsars and active galactic nuclei (AGN).

The study of phenomena related to the amplitude modulation of nonlinear waves propagating in dispersive media,[20,21] such as modulational instability, harmonic generation, and energy localization via a localized structure formation, generically relies on nonlinear-Schrödinger (NLS)-type equations.[22] A set of coupled equations of this kind naturally occurs when the interaction between modulated

[a]Electronic mail: ioannis@tp4.rub.de; http://www.tp4.rub.de/~ioannis
[b]Electronic mail: ps@tp4.rub.de; http://www.tp4.rub.de/~ps
[c]Electronic mail: gem@mpe.mpg.de

waves is considered; their structure (often asymmetric) reflects the particular aspects of the physical problem considered. Coupled NLS equations, such as the ones derived and analyzed here, occur in a variety of self-focusing, self-trapping, and localization-related phenomena, in physical contexts as diverse as electromagnetic wave propagation in nonlinear media,[23,24] optical fibers,[25,26] Langmuir plasma waves,[27] transmission lines,[28] and more recently Bose-Einstein condensates[29] and left-handed metamaterials.[30,31] Our results are qualitatively reminiscent of the findings in those studies. However, the intrinsic structure of our equations (in particular, the form of the nonlinearity coefficients therein), which hinted no specific symmetry (as was often the case in different contexts), required new treatment; thus our results are interesting from a wider perspective (beyond plasma physics).

In this paper, we are interested in studying the parametric coupling between two large-amplitude, magnetic-field-aligned, circularly polarized EMEC waves and ponderomotively driven quasistationary density perturbations. A pair of coupled time-dependent cubic nonlinear Schrödinger equations (CNLSEs) are obtained, describing the spatio-temporal evolution of the modulated EMEC electric-field envelopes. The CNLSEs are used to investigate the occurrence of modulational instability as well as the formation of dark and gray envelope soliton solutions. Explicit profiles for these solutions are presented, and the relevance of our investigation to space plasmas will be discussed.

II. THE MODEL

We consider a uniform collisionless plasma consisting of ions (denoted by "i;" mass m_i, charge $q_i=+e$; e denotes the absolute value of the electron charge) and electrons (mass m_e, charge $q_e=-e$), which is embedded in an external magnetic field $\mathbf{B}=B_0\hat{\mathbf{z}}$, where B_0 is the strength of the magnetic field and $\hat{\mathbf{z}}$ is the unit vector along the z axis. $n_{i/e,0}$ denotes the ion/electron number density at equilibrium, where overall charge neutrality is assumed.

Let us consider nonlinear couplings between two right-hand circularly polarized EMEC waves, which are associated with an electric field in the form $\mathbf{E}_j=F_j(\hat{\mathbf{x}}+i\hat{\mathbf{y}})\exp(ik_jz-i\omega_jt)+\text{c.c.}$, where $\mathbf{F}_j/2=(E_{x,j},E_{y,j},0)$ ($\hat{\mathbf{x}}$ and $\hat{\mathbf{y}}$ denote the unit vectors along the x and y axes, respectively; the index $j=1,2$, here used here to distinguish the two EMEC waves, will be omitted whenever obvious), and low-phase-velocity [compared to the ion/electron thermal speeds $v_{th,i/e}=(T_e/m_{i/e})^{1/2}$] quasistationary density perturbations in our magnetized plasma. We will adopt a cold plasma approximation for the EMEC waves, assuming that $|\omega-\omega_{c,e}|\gg kv_{th,e}$, where $\omega_{c,e}=|q_e|B_0/m_ec$ denotes the electron gyrofrequency. The EMEC wave frequency is much larger than the ion plasma and ion gyrofrequencies, so that ions do not have time to respond to the EMEC waves.

The EMEC wave frequency ω and the wave number $\mathbf{k}$ are related by the cold plasma relation[1] $n^2=c^2k^2/\omega^2=1+\omega_{p,e}^2/[\omega(\omega_{c,e}\cos\theta-\omega)]$ (where the angle θ, given by $\cos\theta=\mathbf{k}\cdot\hat{\mathbf{z}}/k$, measures the propagation obliqueness with respect to the external field direction). Assuming a high medium refractive index $n=kc/\omega\gg1$, one obtains

$$\omega\approx\frac{c^2k^2\omega_{c,e}\cos\theta}{\omega_{p,e}^2+c^2k^2}. \tag{1}$$

Note that the widely used approximate whistler dispersion relation $\omega\approx c^2k^2\omega_{c,e}\cos\theta/\omega_{p,e}^2$ arises in the long-wavelength limit ($k\ll\omega_{p,e}/c$). In the following, we will consider magnetic-field-aligned propagation, i.e., $\mathbf{k}=k\hat{\mathbf{z}}$ (or $\theta=0$).

The interaction between EMEC waves and quasistationary density perturbations produces an electric-field envelope of the EMEC waves, which obeys a nonlinear Schrödinger-type equation;[11–14] in our case, one obtains a pair of (coupled) equations of the form

$$i\left(\frac{\partial E_j}{\partial t}+v_{g,j}\frac{\partial E_j}{\partial z}\right)+P_j\frac{\partial^2E_j}{\partial z^2}-\Delta\omega_jE_j=0\quad(j=1,2), \tag{2}$$

where

$$v_{g,j}=\omega_j'(k)=\frac{2\omega_j}{k_j}\frac{\omega_{c,e}-\omega_j}{\omega_{c,e}} \tag{3}$$

is the group velocity of the (two) EMEC waves and the group velocity dispersion (GVD) coefficients read as

$$P_j=\frac{\omega_j''(k)}{2}=\frac{v_{g,j}}{2k_j}\frac{\omega_{c,e}-4\omega_j}{\omega_{c,e}}. \tag{4}$$

We remark that EMEC waves are characterized by anomalous (normal) group dispersion, viz., $P_j>0$ ($P_j<0$), if $\omega_j<\omega_{c,e}/4$ ($\omega_j>\omega_{c,e}/4$). The EMEC wave dispersion law is depicted in Fig. 1.

The nonlinear frequency shift $\Delta\omega_j$ is given by

$$\Delta\omega_j\approx-\frac{k_jv_{g,j}}{2}N, \tag{5}$$

where the streaming electron fluid velocity associated with the plasma slow motion is assumed to be much smaller than the group velocity of the EMEC waves. Here $N=\delta n_e/n_0$ denotes the electron density perturbation δn_e scaled over the equilibrium density n_0 (recall that $n_{e,0}\approx n_{i,0}\equiv n_0$, since we assume overall quasineutrality near equilibrium).

The low-frequency plasma slow motion is governed by the electron and ion momentum equations, including the advection and nonlinear Lorentz forces. Quasistationary density perturbations (QSDPs) along the magnetic-field direction are driven by the z component of the nonlinear electron Lorentz force.[13,18] Adding inertialess electron and ion momentum equations for the QSDPs, we then obtain[13]

$$\frac{\partial N}{\partial z}\approx\sum_{l=1}^{2}\frac{\omega_{p,e}^2}{\omega_l(\omega_{c,e}-\omega_l)}\frac{1}{4\pi n_0T}\frac{\partial|E_l|^2}{\partial z}, \tag{6}$$

where $T=T_e+T_i$ (here $T_{e/i}$ denotes the electron/ion temperature; the specific-heat ratios $\gamma_{e/i}$ are unity for the adiabatic plasma variations). The (three) evolution equations (2) and (6) now form a closed system, which describes the simultaneous evolution of the relative plasma density perturbation N and the electric-field amplitude E. One notices in the right-hand side of (6) the appearance of the EMEC ponderomotive

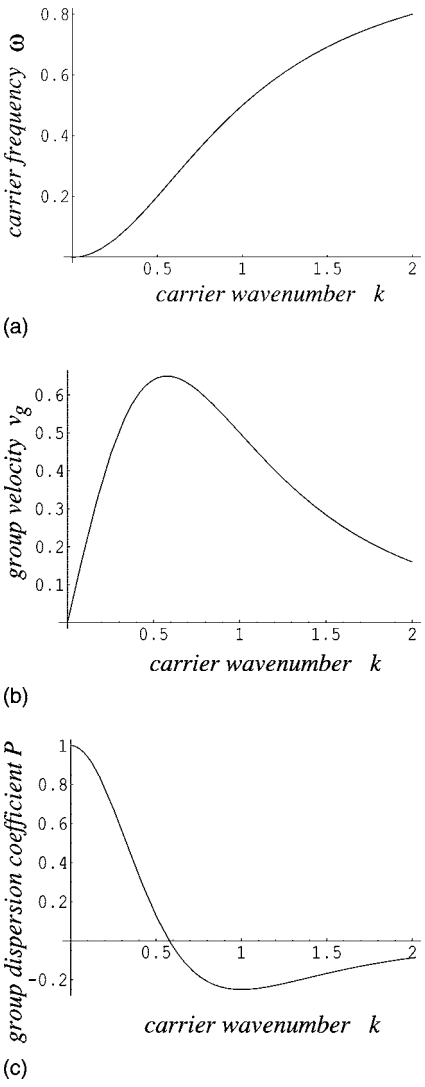

FIG. 1. The dispersion laws of EMEC waves, (a) the wave frequency $\omega(k)$ (scaled by ω_{ce}), (b) the group velocity $v_g=\omega'(k)$ (scaled by $c\omega_{ce}/\omega_{pe}$), and (c) the group-dispersion coefficient $P=\omega''(k)/2$ (scaled by $c^2\omega_{ce}/\omega_{pe}^2$), are depicted vs the wave number k.

force ($\sim|E|^2$) acting on the electrons involved in the plasma slow motion.

Assuming a vanishing density perturbation at infinity, Eq. (6) can be integrated once to obtain the (dimensionless) expression

$$N \approx \sum_{l=1}^{2} \frac{\omega_{p,e}^2}{\omega_l(\omega_{c,e}-\omega_l)} \frac{1}{4\pi n_0 T}(|E_l|^2 - |E_{\infty,l}|^2), \tag{7}$$

where $E_{\infty,l}$ (related to the integration constant) denotes the lth ($l=1,2$) field amplitude at infinity. Now, combining the above expression with (5) we obtain

$$\Delta\omega_j = -\frac{k_j v_{g,j}}{2} \sum_{l=1}^{2} \frac{\omega_{p,e}^2}{\omega_l(\omega_{c,e}-\omega_l)} \frac{1}{4\pi n_0 T}(|E_l|^2 - |E_{\infty,j}|^2)$$

$$\equiv -\sum_{l=1}^{2} Q_{jl}(|\mathcal{E}_l|^2 - |\mathcal{E}_{\infty,l}|^2), \tag{8}$$

where $\mathcal{E}_l = E_l/\sqrt{4\pi n_0 T}$. The definition of the (four) quantities Q_{jl} (for $j,l=1,2$) is obvious, upon inspection. In particular, the self-nonlinearity coefficients, for $l=j$, are given by

$$Q_{jj} = \frac{k_j v_{g,j}}{2} \frac{\omega_{p,e}^2}{\omega_j(\omega_{c,e}-\omega_j)} = \frac{\omega_{p,e}^2}{\omega_{c,e}}, \tag{9}$$

i.e., $Q_{11}=Q_{22}\equiv Q>0$, while the cross-coupling nonlinearity coefficients, for $l\neq j$, read as

$$Q_{jl} = \frac{k_j v_{g,j}}{2} \frac{\omega_{p,e}^2}{\omega_l(\omega_{c,e}-\omega_l)} = \frac{\omega_j}{\omega_l} \frac{\omega_{c,e}-\omega_j}{\omega_{c,e}-\omega_l} \frac{\omega_{p,e}^2}{\omega_{c,e}}. \tag{10}$$

Notice that $Q_{12}Q_{21}=\omega_{p,e}^4/\omega_{c,e}^2\equiv Q^2$ (i.e., $Q_{21}=Q^2/Q_{12}\equiv Q^2/Q'$). Interestingly, the nonlinearity coefficients satisfy

$$Q_{11}Q_{22} - Q_{12}Q_{21} = 0, \tag{11}$$

a property whose importance will be outlined below.

The set of equations in (2) can now be cast in the form of the CNLSEs

$$i\left(\frac{\partial\mathcal{E}_1}{\partial t} + v_{g,1}\frac{\partial\mathcal{E}_1}{\partial z}\right) + P_1\frac{\partial^2\mathcal{E}_1}{\partial z^2} + Q_{11}|\mathcal{E}_1|^2\mathcal{E}_1 + Q_{12}|\mathcal{E}_2|^2\mathcal{E}_1 = 0,$$

$$i\left(\frac{\partial\mathcal{E}_2}{\partial t} + v_{g,2}\frac{\partial\mathcal{E}_2}{\partial z}\right) + P_2\frac{\partial^2\mathcal{E}_2}{\partial z^2} + Q_{22}|\mathcal{E}_2|^2\mathcal{E}_2 + Q_{21}|\mathcal{E}_1|^2\mathcal{E}_2 = 0, \tag{12}$$

where a constant contribution to the left-hand side, related to the value of E_j at infinity, was omitted; in fact, it can be readily eliminated at any stage via a linear phase-shift transformation, namely, $\mathcal{E}_j\to\mathcal{E}_j\exp(i\Sigma_l Q_{jl}|\mathcal{E}_{\infty,l}|^2 t)$. Notice that by "switching off" the coupling (viz., $Q_{ij}\to 0$ or $\mathcal{E}_2\to 0$), the known single EMEC wave limit[18] is exactly recovered, as intuitively expected.

Important information can be obtained by investigating the CNLS equations (12). First, notice that they are symmetric with respect to the permutation $1\leftrightarrow 2$, as physically expected (since the two waves are indistinguishable so far). The sign of the coefficients is crucial in the following. Since $\omega<\omega_{c,e}$, the nonlinearity coefficients Q_{ij} are all (four) *positive* real numbers (in fact functions of k_j, as far as $Q_{jj'}$ are concerned). On the other hand, the dispersion coefficients P_j will (regardless of one another) be positive/negative for a frequency ω_j below/above $\omega_{c,e}/4$ (cf. definitions above), i.e., for wave numbers k_j below/above a threshold k_{ZDP}, which defines the zero-group-dispersion point (ZDP), viz., $P_j(k_j=k_{\mathrm{ZDP}})=0$; the latter is related to the inverse plasma skin length as $k_{\mathrm{ZDP}}=\omega_{p,e}/c\sqrt{3}$. One may readily verify that the frequency for $k=k_{\mathrm{ZDP}}$ is equal to $\omega_{\mathrm{ZDP}}=\omega_{ce}/4$ while the group velocity attains its maximum value $v_{g,\max}=(3\sqrt{3}/8)c\omega_{ce}/\omega_{pe}$. This dispersion law is depicted in Fig. 1.

In the following, we shall investigate the modulational (in)stability of coupled EMEC waves. We shall show that the stability profile is essentially related to the sign of the GVD coefficient P_j, and will then proceed by investigating the effect of the interaction on the EMEC wave stability.

III. UNCOUPLED EMEC WAVES: STABILITY ANALYSIS AND ENVELOPE STRUCTURES

It may be instructive to review the stability analysis and relevant results obtained for the uncoupled case,[18] which is obtained, say, by setting $\mathcal{E}_{j'}$ ($j' \neq j$, any of 1 and 2) to zero in Eqs. (12). Making use of the generic NLS formalism, discussed in detail elsewhere (see, e.g., in Refs. 20 and 22), one expects the electric-field envelope E_j (in the absence of its counterpart E_j') to be *modulationally unstable* if P_j is positive, i.e., if $\omega_j < \omega_{c,e}/4$. To see this, one may first check that the (single here) NLS equation obtained from (12) is satisfied by the plane-wave solution $\mathcal{E}_j(z,t) = \mathcal{E}_0 e^{iQ_{jj}|\mathcal{E}_0|^2 T}$ + c.c. The standard (linear) stability analysis then shows that a linear modulation with frequency Ω and wave number K obeys the dispersion relation

$$(\Omega - v_{g,j}K)^2 = P_j K^2 (P_j K^2 - 2Q_{jj}|\mathcal{E}_0|^2), \tag{13}$$

which exhibits a purely growing amplitude mode if $K \leqslant K_{\mathrm{cr},0} = (2Q_{jj}/P_j)^{1/2}|\mathcal{E}_0|$. The growth rate $\sigma = \mathrm{Im}\,\Omega$ attains a maximum value $\sigma_{\max} = Q_{jj}|\mathcal{E}_0|^2$. For $P_j < 0$, on the other hand, i.e., if $\omega > \omega_{c,e}/4$, the wave is modulationally stable, as is evident from (13).

The (single) NLS equation is an integrable dynamical system[22] which admits, among others, localized solutions in the form of *envelope solitons* of the *bright* or *dark* (*black/gray*) type (for P_j positive or negative, respectively, in our case). Analytical expressions for these solutions are found by inserting the trial function $\mathcal{E} = \mathcal{E}_0 \exp(i\Theta)$ and then separating the real and imaginary parts in order to determine the (real) functions $\mathcal{E}_0(s,\tau)$ and $\Theta(s,\tau)$. Details on the derivation of their analytic form can be found in Refs. 32 and 33, so the final expressions (cf. Ref. 18) need not be derived here. Let us retain that this ansatz amounts to a total electric field whose components $\mathcal{E}_{x/y,j}(z,t)$ are essentially equal to $2\mathcal{E}_0 \cos(kz - \omega t + \Theta)$, where the localized field envelope amplitude ε_0 and the (small) phase shift Θ will be determined, case by case. Once the electric field form is determined, the (copropagating) density perturbation N is then readily given by (7), viz., $N = \alpha(|\mathcal{E}|^2 - |\mathcal{E}_\infty|^2)$, where α is a real (positive here) constant (cf. the appropriate definitions above).

Summarizing, for wave numbers below (above) the critical value $k_0 = \omega_{p,e}/c\sqrt{3}$, where P_{jj} is positive (negative), the single EMEC wave is unstable (stable) and may propagate in the form of a bright- (dark-) type modulated envelope wave packet, i.e., a localized envelope hump against an elsewhere vanishing (constant) wave background; this electric-field excitation is associated with a background density peak (hump), i.e., a copropagating region of increasing (decreasing) density. This behavior is depicted, e.g., in Ref. 18 (see Figs. 1–4 therein).

IV. COUPLED EMEC WAVES: STABILITY ANALYSIS

Let us now consider the complete pair of electric-field envelope functions $E_{1/2}$, whose evolution obeys the coupled NLS equations (12) above. In order to investigate the coupled EMEC wave stability, we shall first seek an equilibrium state by inserting the ansatz $\mathcal{E}_j = \mathcal{E}_{j0} \exp[i\varphi_j(t)]$, where $\mathcal{E}_{j0}$ is a (constant, real) amplitude and $\varphi_j(t)$ is a (real) phase, into Eqs. (12). We thus find a monochromatic (fixed-frequency) solution of the form $\varphi_j(t) = \Omega_{j0} t$, where

$$\Omega_{j0} = Q_{jj}\mathcal{E}_{j0}^2 + Q_{jl}\mathcal{E}_{l0}^2 \quad \text{for } j \neq l = 1,2.$$

Let us consider a small perturbation around the stationary state defined above by taking $\mathcal{E}_j = (\mathcal{E}_{j0} + \epsilon\mathcal{E}_{j1})\exp[i\varphi_j(t)]$, where $\mathcal{E}_{j1}(\mathbf{r},t)$ is a small ($\epsilon \ll 1$) amplitude perturbation of the slowly varying modulated field amplitudes, and $\varphi_j(t)$ is the phasor defined above. Substituting into Eqs. (12) and separating the real and imaginary parts by writing $\mathcal{E}_{j1} = a_j + ib_j$ ($a_j, b_j \in \Re$) and $\mathcal{E}_{1/2,0} = \psi_{1/2,0}$, the first-order terms (in ϵ) yield

$$\begin{aligned} &-\frac{\partial b_j}{\partial t} - v_{g,j}\frac{\partial b_j}{\partial z} + P_j\frac{\partial^2 a_j}{\partial z^2} + 2Q_{jj}\psi_{j0}^2 a_j + 2Q_{jl}\psi_{j0}\psi_{l0}a_l = 0, \\ &\frac{\partial a_j}{\partial t} + v_{g,j}\frac{\partial a_j}{\partial z} + P_j\frac{\partial^2 b_j}{\partial z^2} = 0, \end{aligned} \tag{14}$$

where j and l ($\neq j$) $= 1,2$ (this will henceforth be understood unless otherwise stated). Eliminating b_j, these equations yield

$$\begin{aligned} &\left[\left(\frac{\partial}{\partial t} + v_{g,j}\frac{\partial}{\partial z}\right)^2 + P_1\left(P_1\frac{\partial^2}{\partial z^2} + 2Q_{11}\psi_{10}^2\right)\frac{\partial^2}{\partial z^2}\right]a_1 \\ &\quad + P_1 Q_{12}|\psi_{10}||\psi_{20}|\frac{\partial^2}{\partial z^2}a_2 = 0 \end{aligned} \tag{15}$$

(along with a symmetric equation, obtained by permuting $1 \leftrightarrow 2$). We now let $a_j = a_{j0}\exp[i(Kz - \Omega t)]$ + c.c., where $\mathbf{k}$ and Ω_k are the wave vector and the frequency of the modulation, respectively, viz., $\partial/\partial t \to -i\Omega$ and $\partial/\partial z \to iK$, i.e., $\partial^2/\partial t^2 \to -\Omega^2$ and $\partial^2/\partial z^2 \to -K^2$. After some algebra, we obtain a nonlinear dispersion relation of the form

$$[(\Omega - v_{g,1}K)^2 - \Omega_1^2][(\Omega - v_{g,2}K)^2 - \Omega_2^2] = \Omega_c^4 \tag{16}$$

(the quantities $\Omega_{1,2,c}$ will be defined below), which is essentially a fourth-order polynomial equation in K. For the sake of analytical tractability, we shall henceforth assume equal group velocities, since we are interested in the dynamics near the zero-group-dispersion point, hence $v_{g,1} \approx v_{g,2} \approx \omega'(k_{\mathrm{ZDP}})$. Thus, neglecting the group velocity mismatch (which could have straightforwardly been eliminated in the CNLS equations via a Galilean transformation), we obtain the eigenvalue problem $\mathbf{Ma} = \omega^2\mathbf{a}$, where $\mathbf{a} = (a_1, a_2)^T$ is the vector of the (real part of the) perturbation amplitudes, and the matrix elements are given by $M_{jj} = P_j K^2(P_j K^2 - 2Q_{jj}|\psi_{j0}|^2) \equiv \Omega_j^2$ and $M_{jl} = -2P_j Q_{jl}|\psi_{j0}||\psi_{l0}|K^2$ (for $l \neq j$, both equal to 1 or 2). The frequency Ω and the wave number K are therefore related by the reduced nonlinear dispersion relation

$$(\Omega^2 - \Omega_1^2)(\Omega^2 - \Omega_2^2) = \Omega_c^4, \tag{17}$$

where the coupling is expressed via $\Omega_c^4 = M_{12}M_{21}$ in the right-hand side of Eq. (17).

The nonlinear dispersion relation (17) takes the form of a biquadratic polynomial equation

$$\Omega^4 - T\Omega^2 + D = 0, \tag{18}$$

where $T=\mathrm{Tr}\,\mathbf{M}\equiv\Omega_{11}^2+\Omega_{22}^2$ and $D=\mathrm{Det}\,\mathbf{M}\equiv\Omega_{11}^2\Omega_{22}^2-\Omega_c^4$ are related to the trace and the determinant, respectively, of the matrix $\mathbf{M}$. Equation (18) admits the solution

$$\Omega^2 = \frac{1}{2}[-T \pm (T^2-4D)^{1/2}], \tag{19}$$

or

$$\Omega_\pm^2 = \frac{1}{2}(\Omega_1^2+\Omega_2^2) \pm \frac{1}{2}[(\Omega_1^2-\Omega_2^2)^2+4\Omega_c^4]^{1/2}. \tag{20}$$

We note that the right-hand side is real here, since the discriminant quantity $\Delta=T^2-4D=(\Omega_1^2-\Omega_2^2)^2+4\Omega_c^4$ is a positive quantity here, as one may readily check.

Stability is ensured (for any wave number $\mathbf{k}$) if (and only if) *both* solutions $\Omega_\pm^2$ are *positive real* numbers. Recalling that the sum and the product of the (real, since $\Delta>0$) roots of the polynomial $p(x)=x^2-Tx+D$ is given by T and D, respectively, the stability requirement is tantamount to the following conditions being satisfied simultaneously: $T>0$ *and* $D>0$. One thus has to investigate two distinct polynomial inequalities; note that T and D are *even*-order polynomials of k.

First, the sign of $T=k^2[k^2\Sigma_j P_j^2-2\Sigma_j P_j Q_{jj}|\psi_{j0}|^2]$ (see definitions above) depends on (the sign of) the quantity $\Sigma_j P_j Q_{jj}|\psi_{j0}|^2$ which has to be *positive* for all k in order for stability to be ensured (for any ψ_{j0} and k). Given that $Q_{11}=Q_{22}>0$ this requires that

$$P_1<0 \quad \text{and } P_2<0. \tag{21}$$

Otherwise, T becomes negative (viz., $\Omega_-^2<0$, at least) for K below a critical value $K_{\mathrm{cr},1}=(2\Sigma_j P_j Q_{jj}|\psi_{j0}|^2/\Sigma_j P_j^2)^{1/2}>0$ (cf. the single EMEC criterion above); this is always possible for a sufficiently large perturbation amplitude $|\psi_{20}|$ if, say, $P_2>0$ (even if $P_1<0$). Therefore, only a pair of two stable (individually, i.e., both having $\omega>\omega_{c,e}/4$) EMECs can be stable; the sole presence of a single unstable EMEC may destabilize its counterpart (even if the latter would be individually stable).

Second, $D=\Omega_{11}^2\Omega_{22}^2-\Omega_c^4$ is an eighth-order polynomial in k, which can be factorized as $D=P_1^2P_2^2k^6(k^2-b)$, where $b=2\Sigma_j Q_{jj}|\psi_{j0}|^2/P_j$. Most interestingly, the stability requirement $b<0$ (in order for D to be positive for *any* value of $k>0$ and $|\psi_{j0}|$) here simply amounts to (and is covered by) the criterion (21) above (essentially, this is due to the very structure of Q_{ij}, which satisfies $Q_{11}Q_{22}-Q_{12}Q_{21}=0$ here). If $b>0$, then D becomes negative, and thus instability occurs (since $\Omega_-^2<0$ then), for perturbation wave numbers K below $K_{\mathrm{cr},2}\equiv\sqrt{b}$.

The qualitative consequences of the stability analysis will be briefly explained in the following.

(a) *Destabilization of a stable-unstable EMEC wave pair*. If $P_1>0$ and $P_2<0$, viz., $k_1<k_{\mathrm{ZDP}}<k_2$, then wave 1 (2) would be unstable (stable) individually, i.e., in the absence of its counterpart. The system of coupled EMEC waves will *always* be *unstable* to perturbations with a wave number K below $K_{\mathrm{cr}}=\max\{K_{\mathrm{cr},1},K_{\mathrm{cr},2}\}$ (see definitions above; note that the expressions for $K_{\mathrm{cr},1/2}$ reduces to $K_{\mathrm{cr},0}$—see the definitions in Sec. III—in the single EMEC wave case). However, coupling to wave 2 may yield a slight suppressing effect on the instability of wave 1. This behavior is depicted in Fig. 2, where we have plotted the instability growth rate σ_1 of a single unstable wave 1 (viz., $\sigma_1^2=-\Omega_1^2>0$; upper curve) and that of an unstable-stable EMEC wave pair (viz., $\sigma_1^2=-\Omega_-^2>0$, for $P_1>0>P_2$; lower curve), against the wave number k [both quantities are normalized by their values at the single wave maximum, namely, by $\sigma_0=Q_{11}|\mathcal{E}_{1,0}|^2$ and $K_{\mathrm{cr},0}=(2Q_{11}/P_1)^{1/2}|\mathcal{E}_{1,0}|$, respectively], for two arbitrary choices of parameter values. Both the (coupled EMEC wave) growth rate and critical wave number (below which instability occurs) are seen to *decrease* due to the coupling, as compared to the uncoupled (wave 1 only) case. On the other hand, the maximum of the growth rate also migrates towards higher wavelengths, i.e., lower wave numbers).

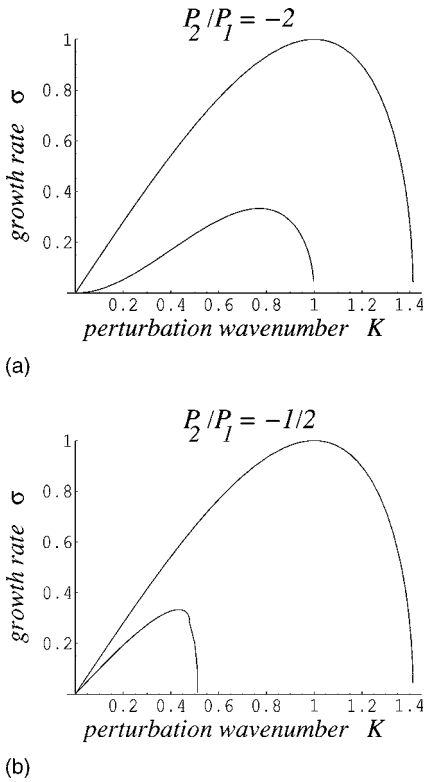

FIG. 2. Unstable-stable EMEC wave coupling. The instability growth rate of a single unstable wave 1, namely, σ_1 (viz., $\sigma_1^2=-\Omega_1^2>0$) (upper curve), and that of an unstable-stable EMEC wave pair (viz., $\sigma_1^2=-\Omega_-^2>0$, for $P_1>0>P_2$) are depicted against the wave number k (normalized by $\sigma_0=Q_{11}|\mathcal{E}_{1,0}|^2$ and $K_{\mathrm{cr},0}=(2Q_{11}/P_1)^{1/2}|\mathcal{E}_{1,0}|$, respectively) for $|\mathcal{E}_{1,0}|=|\mathcal{E}_{2,0}|$ and P_2/P_1 equal to (a) −2 and (b) −1/2.

(b) *Enhanced destabilization of two unstable EMEC waves*. If $P_1>0$ and $P_2>0$, viz., k_1, $k_2<k_{\mathrm{ZDP}}$, then both waves would be unstable individually, in the absence of its counterpart. In this case, the coupled system will be unstable to perturbations with a wave number K below $K_{\mathrm{cr}}=\max\{K_{\mathrm{cr},1},K_{\mathrm{cr},2}\}$ (cf. above). In practical terms, even if one (or both) wave(s) is (are) characterized by a frequency ω *below* $\omega_{c,e}/4$, i.e., by a wave number k below $k_0=\omega_{p,e}/c\sqrt{3}$, then the coupled wave system is *unstable*. As one may verify, either via a tedious analytical investigation or numerically,

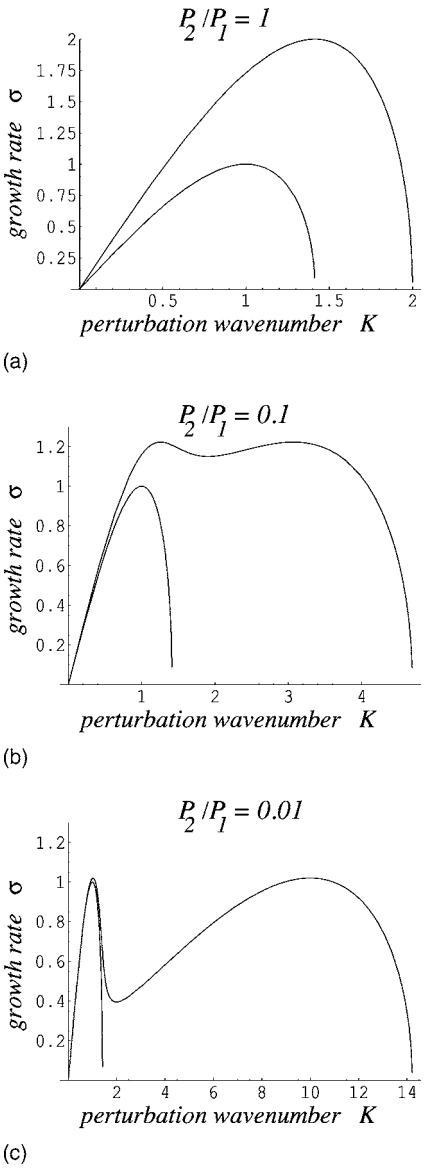

FIG. 3. Unstable-unstable EMEC wave coupling. The instability growth rate σ_1 of a single unstable wave 1, (viz., $\sigma_1=-\Omega_1^2$) (lower curve) and that of an unstable-unstable EMEC wave pair (i.e., $\sigma_1^2=-\Omega_-^2>0$, for P_1, $P_2>0$) are depicted against the perturbation wave number K (normalized by $\sigma_0=Q_{11}|\mathcal{E}_{1,0}|^2$ and $K_{cr,0}=(2Q_{11}/P_1)^{1/2}|\mathcal{E}_{1,0}|$, respectively) for $|\mathcal{E}_{1,0}|=|\mathcal{E}_{2,0}|$ and P_2/P_1 equal to (a) 1, (b) 0.1, and (c) 0.01. Notice the interplay between the two bell-shaped curves predicted by the theory.

coupling between waves 1 and 2 bears an enhancing effect on the instability of both. This can be seen in Fig. 3, where we have depicted the instability growth rate σ_1 of a single unstable wave 1 (viz., $\sigma_1^2=-\Omega_1^2>0$; $P_1>0$; lower curve) and that of an unstable-unstable EMEC wave pair (viz., $\sigma_1^2=-\Omega_-^2>0$, for $P_1>0>P_2$; upper curve), against the wave number k (both quantities are normalized by their values at the single unstable wave maximum, namely, by $\sigma_0=Q_{11}|\mathcal{E}_{1,0}|^2$ and $K_{cr,0}=(2Q_{11}/P_1)^{1/2}|\mathcal{E}_{1,0}|$, respectively), for two arbitrary choices of parameter values. The unstable wave-number region is seen to *expand*, as compared to the uncoupled (wave 1 only) case. The growth rate may attain a maximum value which is increased by a factor of 2 (compared to the uncoupled case), when $P_{1/2}$ bear (positive) values which are similar in magnitude, i.e., when $k_1=k_2\lesssim k_{ZDP}$ (and, say, $|\psi_{10}|=|\psi_{20}|$) [see Fig. 3(a)]. However, the maximum value of the growth rate becomes slightly lower, and the unstable wave-number range goes much wider, when P_2/P_1 attains values much different from unity; this effect is due to the interplay between the two instability regions shown above. This behavior is depicted in Figs. 3(b) and 3(c). Modulational instability is thus dramatically enhanced due to coupling with an EMEC wave near the ZDP (viz., $0<P_2\ll P_1$).

(c) *Stability of two intrinsically stable EMEC waves*. Only if *both* waves have wave numbers $k_{1/2}>\omega_{p,e}/c\sqrt{3}$, viz., $P_{1/2}<0$, i.e., k_1, $k_2>k_{ZDP}$, will the coupled wave pair be stable to external perturbations. A pair of individually stable waves will thus remain stable while interacting with one another. Rather counterintuitively, a previously known feature, e.g., of coupled nonlinear beam propagation, namely, a pair of stable beams being destabilized due to coupling, is not reproduced here; this is due to the structure of the nonlinearity coefficients (see the discussion above).

V. COUPLED MODULATED ENVELOPE EMEC SOLITON EXCITATIONS

The system of coupled NLS equations (12) have been investigated in a number of theoretical works. It was shown to be integrable for a specific choice of parameters, namely, if $Q_{12}/Q_{11}=Q_{21}/Q_{22}=1$,[34,35] when it is solved by the inverse scattering transform;[24] this condition is here fulfilled only if the colliding EMEC waves bear the same wave number $k_1=k_2$. Various types of solutions have been shown to exist, including coupled bright envelope solitons (pulses),[24,27,36] bright-to-dark coupled envelope solitons,[37,38] domain walls (obtained numerically),[39] and cnoidal waves.[40] In the following, we shall briefly review some of the existing analytical results of interest here, with respect to our coupled EMEC wave propagation problem.

A. Bright and dark single (uncoupled) envelope solitons

It may be instructive to consider the single wave (uncoupled) case, which is obtained, say, by setting $\mathcal{E}_2=0$ in Eqs. (12). A stationary soliton solution to the remaining (single) NLS equation may be sought in the form $\mathcal{E}=\exp(iP\mu^2t)\tilde{E}$ (index 1 will be dropped in this paragraph, hence $\tilde{E}=\tilde{E}_1$, $P=P_1$, and $Q=Q_{11}$), where μ is a real constant and $\tilde{E}(z)$ is a real function to be determined. The general "Galilean boosted" soliton solution of the (single) NLS is then given by

$$\mathcal{E}=\exp[i(\tilde{k}z+\tilde{\omega}t+\Theta)]\tilde{E}(z-u_et) \quad \text{(Ref. 32 and 36)}, \tag{22}$$

where u_e is the (arbitrary real) envelope velocity and $\tilde{k}=u_e/2P$, $\tilde{\omega}=P(\mu^2-u_e^2/4P^2)$, and Θ are the small wave number, frequency, and phase (constant) corrections (due to amplitude modulation), to be determined.

For $PQ>0$, one finds the *bright*-type (pulse-shaped) envelope single soliton solution[32,36]

$$\tilde{E}(z) = \pm \left(\frac{2P}{Q}\right)^{1/2} \mu \,\mathrm{sech}(\mu z), \tag{23}$$

which represents a localized envelope pulse confining the fast carrier oscillations. The phase shift Θ is a real (arbitrary) constant. Recalling Eq. (7), we see that a bright electric-field envelope excitation is accompanied by a copropagating positive density variation (a localized density hump) (see Fig. 1 in Ref. 18).

For $PQ<0$, one finds the *black*-type soliton

$$\tilde{E}(z) = \pm \left|\frac{2P}{Q}\right|^{1/2} \mu \tanh(\mu z), \tag{24}$$

which represents a propagating localized region of zero-field value, i.e., a void inside an elsewhere finite oscillation amplitude region. The phase shift Θ is a real (arbitrary) constant.

For $PQ<0$, one also obtains the *gray*-type soliton

$$\tilde{E}(z) = \pm \left|\frac{2P}{Q}\right|^{1/2} \frac{1}{d}\mu[1 - d^2\,\mathrm{sech}^2(\mu z)]^{1/2}, \tag{25}$$

representing a region of reduced (yet nonvanishing) electric-field value (an envelope hole). Here, d is a real number ($|d|\leqslant 1$) which determines the localized electric-field dip at the middle (for $s=z-u_e t=0$). The black soliton (24) is recovered for $d=1$. The phase shift Θ here is a complex (real) function of z and t (Refs. 18 and 32) (omitted here for simplicity). Recalling Eq. (7), we see that both dark (i.e., black or gray) electric-field envelope excitations are accompanied by a copropagating negative density variation (a localized density dip) (see Figs. 3 and 4 in Ref. 18).

Notice that the maximum amplitude $\mathcal{E}_{\max} \sim (2P_1/Q_{11})^{1/2}\mu$ of all these excitations is, in fact, inversely proportional to its spatial extension (width) $L=\mu^{-1}$, i.e., $\mathcal{E}_{\max} L=$const. [unlike Korteweg–de Vries solitons, which formally satisfy $E_{\max} L^2=$const. (see in Ref. 33 for a detailed discussion)].

B. Bright-bright coupled envelope solitons

Coupled soliton solutions to the set of equations in (12) (for $v_{g,1}\approx v_{g,2}$) have been shown (see, e.g., in Refs. 27 and 36) to exist in the form

$$\mathcal{E}_j = \exp[i(\tilde{k}_j z + \tilde{\omega}_j t + \Theta_j)]\tilde{E}_j(z - u_e t)$$
$$\text{(for } j=1,2\text{)} \quad \text{(Ref. 36)}, \tag{26}$$

where $\tilde{k}_j=\xi_j$, $\tilde{\omega}_j=P_j(\mu_j^2-\xi_j^2)$, and Θ_j are the small wave number, frequency, and phase corrections. Here $\mu_{1/2}$ and $\xi_{1/2}$ are real constants and $\tilde{E}_{1/2}(z)$ are real functions of $s=z-u_e t$, to be determined, while u_e is a (coupled) envelope velocity which satisfies $u_e=2P_1\xi_1=2P_2\xi_2$ (hence $\xi_2=\xi_1 P_1/P_2$).

The elementary coupled bright-type (pulse-shaped) envelope solution takes the functional form $\tilde{E}_j(z)=a_j w(x;\mu^2)$ (for $j=1,2$), where the function w satisfies

$$w_{xx} - \mu^2 w + 2w^3 = 0.$$

The solution takes the form[27,36]

$$\tilde{E}_j(z) = \pm\, a_j\mu_j \,\mathrm{sech}(\mu_j z), \tag{27}$$

which represents a pair of localized envelope pulses, confining the fast electric-field oscillations in the two EMEC waves and copropagating at the same speed u_e. The phase shift Θ is a real (arbitrary) constant. The coefficients a_j are, in general, solutions of the linear system[27,36]

$$\frac{Q_{11}}{P_1}a_1^2 + \frac{Q_{12}}{P_1}a_2^2 = \frac{Q_{21}}{P_2}a_1^2 + \frac{Q_{22}}{P_2}a_2^2 = 2. \tag{28}$$

Interestingly, the characteristic determinant here is zero [see (11) above], so these solutions will only exist under the constraint $P_1Q_{11}=P_2Q_{12}$ or $P_1Q=P_2Q'$ (cf. definitions above). Upon substituting from the above definitions, these conditions amount to the requirement $(\omega_{c,e}-4\omega_1)/k_1=(\omega_{c,e}-4\omega_2)/k_2$, which is fulfilled (in combination with $v_{g,1}=v_{g,2}$, as, e.g., in the vicinity of the ZDP) only if $k_1=k_2$. The solutions for a_j then satisfy $Qa_1^2+Q'a_2^2=2P_1$. Now, recalling Eq. (7), we see that this bright-bright bienvelope soliton excitation is accompanied by a copropagating positive density variation, i.e., a localized density hump in the formal form $N=\Sigma_j C_j\,\mathrm{sech}^2(\mu_j z)$; its form is determined by C_j, which are appropriate coefficients, i.e., functions of the parameters μ_1, μ_2, and of $k_1\approx k_2$). The localized-density variation N and the field envelopes $E_{1/2}$ propagate at the same velocity u_e and bear characteristics (relative magnitude and width) which depend on the parameter values. This behavior is shown in Fig. 4, where we have depicted two bright electric-field envelope soliton excitation profiles with $\mu_2>\mu_1$ (thus wave 2 is higher and narrower) versus space s—normalized by the (common) wavelength—in a moving frame. The two envelopes are accompanied by a *positive* copropagating density perturbation N (*density compression*).

C. Bright-dark coupled envelope solitons

Searching for localized excitations characterized by vanishing boundary conditions for one of the waves, say, $\mathcal{E}_1 \to 0$ as $z\to\pm\infty$, and finite ones for the other, viz., $\mathcal{E}_2\to a_2$ as $z\to\pm\infty$, one obtains a set of solutions in the form $\mathcal{E}_j = a_j\tilde{E}_j\exp[i(\xi_j z-\tilde{\omega}_j t+\Theta_j)]$ (for $j=1,2$), with

$$\hat{E}_1 = \mu_1\,\mathrm{sech}[\mu_1(z-u_e t)],$$
$$\hat{E}_2 = \mu_2\{1 - d^2\,\mathrm{sech}^2[\mu_2(z-u_e t)]\}^{1/2}, \tag{29}$$

where, same as above, the parameters μ_j and a_j need to be determined, along with a set of associated criteria for existence; details can be found in Refs. 37 and 38 and are omitted here. The parameters here satisfy[37] $u_e=2P_1\xi_1=2P_2\xi_2$, as in the bright-bright soliton pairs presented above. No such solutions are possible for $P_1<0<P_2$. In combination with Eq. (7) for the associated density variation, we notice that the sign (either positive or negative) of the latter is not prescribed beforehand, since it is essentially determined by (the interplay between) μ_1 and μ_2; to see this, notice in particular that $|\mathcal{E}_2|^2-|\mathcal{E}_{2,\infty}|^2<0<|\mathcal{E}_1|^2-|\mathcal{E}_{1,\infty}|^2$ in this case. Again, the localized-density variation N and the field envelopes $E_{1/2}$ propagate at the same velocity u_e and bear characteristics

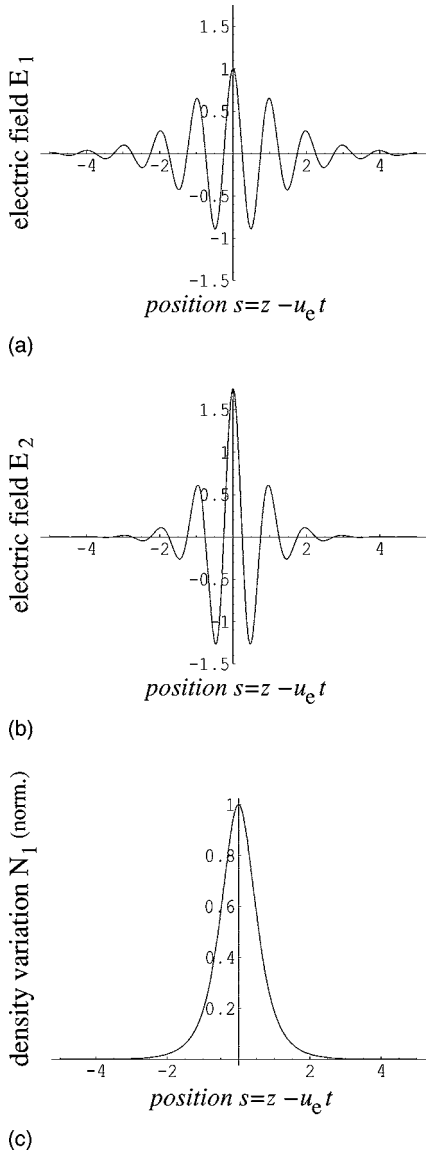

FIG. 4. Bright-bright coupled excitation. The bright-type (pulse-like) EMEC wave electric-field-localized envelope excitations: (a) $E_1(s)$, (b) $E_2(s)$ [both scaled by $E_1(0)$], and (c) the plasma density variation $N_1(s) \sim \Sigma_j C_j(|\mathcal{E}_j|^2 - |\mathcal{E}_{j,\infty}|^2)$ [here scaled by $|N(0)|$; C_j real], as derived from (27) for $C_1 = C_2 = 1$ and $k_1 = k_2$ (otherwise arbitrary values), are depicted against the reduced space variable $2\pi s/\lambda$ (where $s = z - u_e t$). Here we have taken $\mu_2/\mu_1 = 1.75$. Notice that a higher value of μ implies a narrower and taller envelope excitation.

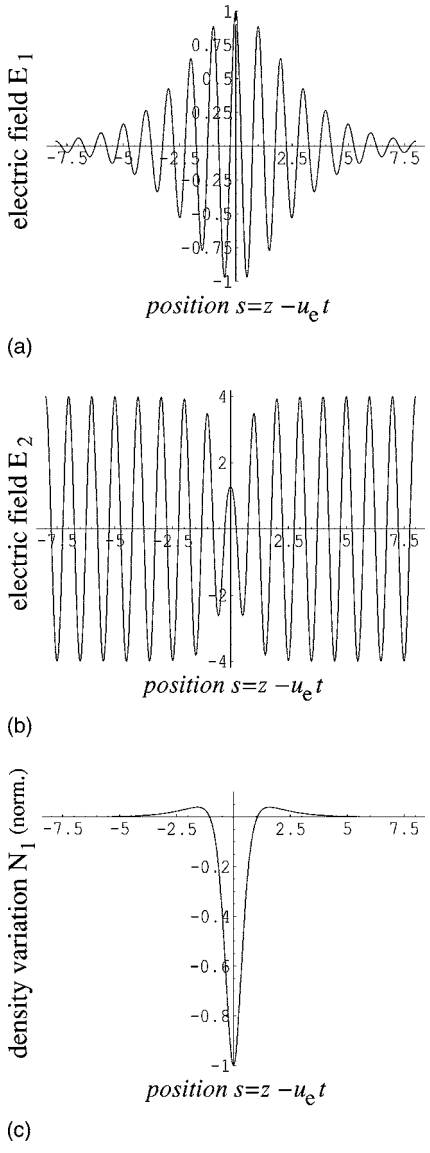

FIG. 5. Bright-dark coupled excitation. (a) The bright-type (pulse-like) EMEC wave 1 electric field $E_1(s)$, (b) its dark-type (void, hole) counterpart for wave 2, $E_2(s)$ [both scaled by $E_1(0)$], and (c) the plasma density variation $N_1(s) \sim \Sigma_j C_j(|\mathcal{E}_j|^2 - |\mathcal{E}_{j,\infty}|^2)$ [here scaled by $|N(0)|$; C_j real], as derived from (29) for $C_1 = C_2 = 1$ and $k_1 = k_2$ (otherwise arbitrary values), are depicted against the reduced space variable $2\pi s/\lambda$ (where $s = z - u_e t$). Here we have taken $\mu_2/\mu_1 = 2/0.5 = 4$. Notice that a higher value of μ implies a narrower and taller envelope excitation. The sign of N varies due to the interplay between μ_1 and μ_2 (otherwise C_1 and C_2 as well), here taken to be equal.

(relative magnitude and width) which depend on the parameter values. This (set of) excitation(s) is depicted in Fig. 5 for a set of (arbitrary) parameter values, with $\mu_2 > \mu_1$—thus the wave 2 electric-field localized variation (void) is narrower that that of wave 1 (field increase, pulse)—versus space s (normalized by a common wavelength) in a moving frame. Since $|\mathcal{E}_2| < |\mathcal{E}_{2,\infty}|$ for the (dark) second excitation (though $|\mathcal{E}_1| > |\mathcal{E}_{1,\infty}| = 0$ for the bright first one), the density variation N which accompanies the two field envelope excitations may either be positive or negative depending on the (values of the) parameters C_j. The latter is the case of Fig. 5, where the two envelopes are accompanied by a negative copropagating density perturbation N (*density rarefaction*).

VI. CONCLUSIONS

In this paper, we have presented an investigation of the behavior of nonlinearly coupled magnetic-field-aligned EMEC waves which have different group dispersions near $\omega_j \sim \omega_{c,e}/4$. The nonlinear coupling between the two EMEC waves occurs due to quasistationary density perturbations that are driven by the combined action of the ponderomotive force of two EMEC waves in magnetized plasmas. Due to this nonlinear interactions, we obtain a closed set of evolution equations for the modulated electric-field amplitudes $\mathcal{E}_1$ and $\mathcal{E}_2$ of the EMEC waves, and the relative plasma density variation $N = n_1/n_0$, which was then reduced to a pair of coupled nonlinear Schrödinger equations for the EMEC

waves. The modulational stability analysis around a steady state of two coupled harmonic waves has shown that a pair of coupled EMEC waves may become unstable unless both waves were individually stable. Although the preceding analysis was explicitly limited in the region neighboring the zero-group-dispersion point, where the modulated electric-field envelope dispersions (related to the curvature of the carrier wave's dispersion relation) change sign (from positive to negative), the results obtained are presumably valid in a wider range of the carrier wave-number values; this hypothesis may be investigated by a complicated analytical and numerical analysis of the full (fourth-order polynomial) perturbation dispersion relation (16), a tedious task which goes beyond the scope of this paper.

The results presented here are of relevance to recent observations in space[3,4,8] and laboratory[5,7,8] plasmas, where such phenomena are clearly observed. A complete theory for the formation and dynamics of envelope EMEC structures has always been lacking in the literature, so the present study aims at contributing to filling this gap.

ACKNOWLEDGMENTS

One of the authors (I.K.) is grateful to the Max-Planck-Institut für extraterrestrische Physik (Garching, Germany) for the award of a fellowship (project: "Complex Plasmas").

This work was partially supported by the Deutsche Forschungsgemeinschaft (Bonn, Germany) through the Sonderforschungsbereich (SFB) 591—Universelles Verhalten Gleichgewichtsferner Plasmen: Heizung, Transport und Strukturbildung.

[1] T. Stix, *Waves in Plasmas* (American Institute of Physics, New York, 1992).
[2] W. Baumjohann and R. A. Treumann, *Basic Plasma Space Physics* (Imperial College Press, London, 1996).
[3] O. Moullard, A. Masson, H. Laakso, M. Parrot, P. Decreau, O. Santolik, and M. Andre, Geophys. Res. Lett. **29**, 1975 (2002).
[4] G.-L. Huang, D.-Y. Wang, and Q.-W. Song, J. Geophys. Res. **109**, A02307 (2004).
[5] R. L. Stenzel, Phys. Fluids **19**, 857 (1976).
[6] J. F. Bamber, J. E. Maggs, and W. Gekelman, J. Geophys. Res. **100**, 23795 (1995).
[7] A. V. Kostrov, M. E. Gushchin, S. V. Korobkov, and A. V. Strikovskii, JETP Lett. **78**, 1026 (2003).
[8] R. L. Stenzel, J. Geophys. Res. **104**, 379 (1999).
[9] A. Hasegawa, Phys. Rev. A **1**, 1746 (1970).
[10] A. Hasegawa, Phys. Fluids **15**, 870 (1972).
[11] V. I. Karpman and H. Washimi, Zh. Eksp. Teor. Fiz. **71**, 1010 (1976) [Sov. Phys. JETP **44**, 528 (1976).
[12] V. I. Karpman and H. Washimi, J. Plasma Phys. **18**, 173 (1977).
[13] P. K. Shukla and L. Stenflo, Phys. Rev. A **30**, 2110 (1984).
[14] N. N. Rao and P. K. Shukla, Phys. Plasmas **4**, 636 (1997).
[15] N. N. Rao and P. K. Shukla, Phys. Lett. A **243**, 151 (1998).
[16] P. K. Shukla, L. Stenflo, R. Bingham, and B. Eliasson, Plasma Phys. Controlled Fusion **46**, B349 (2004).
[17] B. Eliasson and P. K. Shukla, Geophys. Res. Lett. **31**, L17802 (2004).
[18] I. Kourakis and P. K. Shukla, Phys. Plasmas **12**, 012902 (2005).
[19] T. Cattaert, I. Kourakis, and P. K. Shukla, Phys. Plasmas **12**, 012319 (2005).
[20] A. Hasegawa, *Plasma Instabilities and Nonlinear Effects* (Springer, Berlin, 1975).
[21] M. Remoissenet, *Waves Called Solitons* (Springer, Berlin, 1994).
[22] C. Sulem and P. L. Sulem, *The Nonlinear Schrödinger Equation* (Springer, Berlin, 1999).
[23] L. A. Ostrovskii, Zh. Eksp. Teor. Fiz. [Sov. Phys. JETP **24**, 797 (1967)].
[24] S. V. Manakov, Zh. Eksp. Teor. Fiz. [Sov. Phys. JETP **38**, 248 (1974)].
[25] A. Hasegawa and F. Tappert, Appl. Phys. Lett. **23**, 142 (1973).
[26] G. Agrawal, P. L. Baldeck, and R. R. Alfano, Phys. Rev. A **39**, 3406 (1989).
[27] M. R. Gupta, B. K. Som, and B. Dasgupta, J. Plasma Phys. **25**, 499 (1981).
[28] J. M. Bilbault, P. Marquie, and B. Michaux, Phys. Rev. E **51**, 817 (1995).
[29] K. Kasamatsu and M. Tsubota, Phys. Rev. Lett. **93**, 100402 (2004).
[30] N. Lazarides and G. P. Tsironis, Phys. Rev. E **71**, 036614 (2005).
[31] I. Kourakis and P. K. Shukla, "Nonlinear propagation of electromagnetic waves in negative refraction index composite materials," Phys. Rev. E (in press).
[32] R. Fedele and H. Schamel, Phys. Scr. **T98**, 18 (2002).
[33] R. Fedele, Phys. Scr. **65**, 502 (2002).
[34] R. Sahadevan, K. M. Tamizhmani, and M. Lakshmanan, J. Phys. A **19**, 1783 (1986).
[35] R. Radhakrishnan, R. Sahadevan, and M. Lakshmanan, Chaos, Solitons Fractals **5**, 2315 (1995).
[36] B. Tan and J. P. Boyd, Chaos, Solitons Fractals **T11**, 1113 (2000).
[37] S. V. Vladimirov, L. Stenflo, and M. Y. Yu, Phys. Lett. A **153**, 144 (1991).
[38] M. Lisak, A. Höök, and D. Anderson, J. Opt. Soc. Am. B **7**, 810 (1990).
[39] M. Haelterman and A. P. Sheppard, Phys. Lett. A **185**, 265 (1994).
[40] F. T. Hioe, Phys. Rev. Lett. **82**, 1152 (1991).